JACS
JOURNAL OF THE AMERICAN CHEMICAL SOCIETY
Communication
pubs.acs.org/JACS

Conformation Modulated Optical Activity Enhancement in Chiral Cysteine and Au Nanorod Assemblies

Bing Han,[†] Zhening Zhu,[†] Zhengtao Li,[†] Wei Zhang,*[,‡] and Zhiyong Tang*[,†]

[†]Laboratory of Nanomaterials, National Center for Nanoscience and Technology, Beijing 100190, P. R. China
[‡]Institute of Applied Physics and Computational Mathematics, Beijing 100088, P. R. China

Supporting Information

ABSTRACT: Assemblies of chiral cysteine (CYS) and Au nanorods (GNRs) are constructed in two typical patterns, end-to-end and side-by-side. Impressively, side-by-side assembled GNRs with CYS show obviously stronger plasmonic circular dichrosim (CD) response compared with the end-to-end assemblies. The corresponding theoretical calculation elucidates the intrinsic relationship among geometric structure, electromagnetic interaction, and induced plasmonic CD of the assemblies. This work will significantly benefit the design and application of plasmonic nanodevices with controllable chiroptical responses.

Optical activity characterization, especially based on circular dichroism (CD) spectrum, is believed to be one of the most powerful tools to examine the conformational transitions of biomolecules.[1] Recent studies further demonstrate that conjugation of noble metal nanoparticles (NPs) with chiral molecules could switch the optical activity, which is usually located in the UV light range for conventional molecular chirality, to the visible wavelength region.[2] This new CD response located at the frequency of surface plasmonic resonance (SPR) band of the noble metal NPs is termed as plasmonic CD, which originates from the Columbic interaction between the noble metal NPs and the chiral absorbers.[3] More interestingly, such plasmonic responses might be remarkably amplified with construction of three-dimensional (3D) noble metal NP assemblies of varying arrangements,[4] where the radiative plasmon−plasmon interaction between NPs is responsible for CD enhancement.[5] Thanks to better sensitivity and reliability of the visible optical measurements compared to the UV ones, the NP assemblies with enhanced plasmonic response hold many application opportunities in photonics,[6] sensing,[7] enantioselective separation,[8] and biological diagnosis.[9]

It should be pointed out that the existent experimental design and theoretical studies have mostly focused on the simple models with spherical NPs or NP oligomers.[3,4] Compared with spherical NPs, the anisotropic noble metal NPs like Au nanorods (GNRs) possess two distinct SPR bands, and moreover they are easily assembled to form spatial chirality, e.g., noncentrosymmetric structures formed by GNR dimers.[10] All these characteristics allow GNRs to become excellent candidates to produce strong plasmonic CD responses, which have been confirmed by recent experiments.[11] However, understanding and manipulating the plasmonic CD responses of GNR assemblies still remains difficult because either the mutual orientation or the interparticle distance between the anisotropic GNRs is likely to vary largely in the assemblies. Therefore, it is imperative to develop reliable model systems for exploration of the key factors that influence the optical activity of GNR assemblies. Herein, chiral cysteine (CYS) and GNRs are intentionally assembled in typical end-to-end (EE) and side-by-side (SS) modes. Conformation modulated plasmonic CD enhancement is observed. Both experimental result and theoretical calculation reveal that the conformation-dependent enhancement of plasmonic CD responses is attributed to the change in the electromagnetic interactions between GNRs in the assemblies.

The different assembly modes are realized through changing the concentration of cetyltrimethylammonium bromide (CTAB) surfactants in GNR solution, while the concentration of the added CYS is fixed at 10 μM (see SI for the experimental details). Our experiments showed that if the concentration of CTAB in solution was <7 μM, addition of CYS would result in random aggregation of GNRs. This phenomenon is reasonable because GNRs could not be stabilized by small amount of CTAB surfactants. Subsequently, pH value of the GNR solution was adjusted to 6.3, which was higher than the isoelectric point of CYS molecules, endowing the negative charge nature of CYS in the solution. CYS then assembled with GNRs through electrostatic attraction with positively charged CTAB on GNR surfaces.[12] The assembly behavior of GNRs with CYS in the solution containing different concentration of CTAB is identified by UV−vis absorption and CD spectra. Figures 1 and S2 present a typical

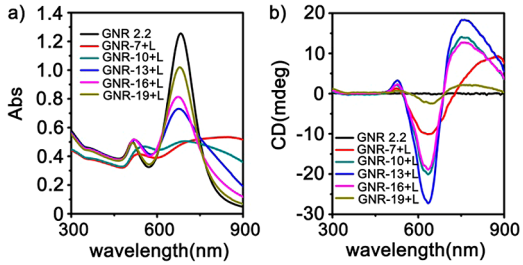

Figure 1. (a) UV−vis and (b) CD spectra of original GNRs (black curves) with aspect ratio of ~2.2 and L-CYS assembled GNRs under different CTAB concentrations. The numbers in the labels correspond to the CTAB concentration in the system, e.g., GNR-7+L stands for the L-CYS-GNR assembly in solution containing 7 μM CTAB.

Received: July 6, 2014
Published: October 27, 2014

dx.doi.org/10.1021/ja506790w | J. Am. Chem. Soc. 2014, 136, 16104−16107

assembly case of GNRs with an average aspect ratio of ∼2.2. As shown by the red curve in Figure 1a, at a low CTAB concentration of 7 μM, the intensity of the longitudinal SPR (LSPR) absorption peak is dramatically reduced upon addition of L-CYS, while a new absorption shoulder at 850 nm appears. This is the typical feature of the EE GNR assembly.[13] When the concentration of CTAB increases to 13 μM (blue curve in Figure 1a), addition of CYS results in both intensity reduction and blue shift of LSPR peak (from 682 to 671 nm), which is the characteristic of SS assembled GNRs.[13] As the CTAB concentration further increases, the intensity of the LSPR peaks is instead improved, and the peak position is red-shifted (pink and yellow curves in Figure 1a), implying that the degree of SS assembly is gradually reduced. Direct observation by scanning electron microscope (SEM) imaging (Figure 2a–f), transmission electron microscopy

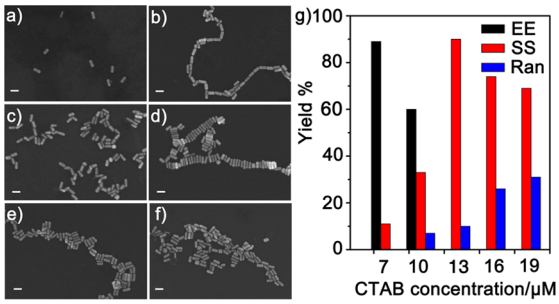

Figure 2. Representative SEM images of (a) original GNRs and the L-CYS assembled GNRs under different CTAB concentrations: (b) 7, (c) 10, (d) 13, (e) 16, (f) 19 μM; scale bar = 50 nm. (g) Statistic distribution of different assembly modes of L-CYS-GNRs formed under different CTAB concentrations. EE, SS, and Ran represent end-to-end, side-by-side and random arrangement, respectively.

(TEM) imaging (Figure S2), and the corresponding statistic analysis (Figure 2g) also confirms the transition of GNR assemblies from EE to SS dominated mode.

The reason for CTAB concentration determining assembly modes is elucidated as follows: When the CTAB concentration in solution is only 7 μM, the added CYS molecules (10 μM) are excessive. So the electrostatic attraction between CYS and CTAB in solution causes the result that kinetic adsorption of CTAB stabilizers on GNR surfaces is not enough, and the CTAB bilayers at the ends of GNRs become less ordered and loose.[14] As a result, the ends of GNRs become high-energy positions, favoring enrichment of considerable numbers of CYS molecules and leading to formation of EE assemblies. On the contrary, when the CTAB concentration increases to 13 μM, CTAB becomes excessive with respect to CYS. The extra CTAB surfactants are enough to kinetically stabilize whole GNRs, eliminating the energy difference between the sides and ends of GNRs toward adsorption of CYS molecules. Owing to the larger surface area, the chance of the attachment of CYS molecules to the sides of GNRs, with respect to the ends of GNRs, is much higher, which thus induces SS GNR assemblies. We also notice that in the SS GNR assemblies, since most CYS molecules electrostatically interact with excessive CTAB in solution, the number of adsorbed CYS molecules in the SS GNR assemblies should be less. This deduction is supported by the fact that the total quantity of CYS attached on the GNRs in SS assembly is smaller than that in EE mode (Table S1). Notably, under the condition of 7 or 13 μM CTAB, GNRs involved in EE or SS assemblies can reach ∼90%, respectively, which provides an ideal model system to study the relationship between the conformation and optical activity of GNR assemblies (Figures 1 and 2).

CD survey indicates that both EE and SS assemblies of GNRs possess three CD peaks near the frequency of SPR bands: one at 480−550 nm corresponding to transverse SPR (TSPR) absorption and two in the region of 550−900 nm attributing to LSPR absorption (Figure 1b). These plasmonic CD peaks originate from the chiral currents inside the GNRs induced by the dipole of the chiral molecule (L-CYS) upon formation of the L-CYS and GNR hybrids. The strong bisignated CD peaks corresponding to LSPR absorption are related to splitting of the excited-state levels via assembly, which has been clarified in recent studies.[11a,b] Very interestingly, although these two types of GNR assemblies show similar CD line shape, there are several significant differences resulting from the different arrangement of GNRs. First, SS assembled GNRs experiences less CD peak shift than EE assembled GNRs, which is consistent with the plasmon hybridization theory of GNRs.[13,15] Second, at the CTAB concentration of 13 μM, GNRs adopt SS arrangement to the largest extent and exhibit considerable CD enhancement compared with the EE assembly. The anisotropic factor (g factor) of the negative CD peak corresponding to the LSPR absorption is used for quantitative comparison (see page S14 in SI for the definition and calculation details of g factor). The g factor of the SS assembled GNRs ($\sim 15.17 \times 10^{-4}$) is 2 times larger than that of the EE assembled GNRs ($\sim 7.49 \times 10^{-4}$) (Table 1). Lastly,

Table 1. Comparison between the Experimental and Theoretical Results of Anisotropic Factors (g_{EE} and g_{SS}) of CD Peaks Corresponding to LSPR of EE and SS Assembled GNRs with Different Aspect Ratio

	LSPR negative CD peak					
	$g_{EE} \times 10^{-4}$		$g_{SS} \times 10^{-4}$		enhancement factor[a]	
aspect ratio	exp.	theor.	exp.	theor.	exp.	theor.
2.2	−7.49	−7.22	−15.17	−14.98	2.00	2.07
2.9	7.54	−7.34	−24.52	−28.67	3.25	3.90
3.4	−9.61	−9.80	−55.70	−55.36	5.85	5.65

[a]Enhancement factor is defined as the ratio of g_{SS} to g_{EE}.

as the degree of SS assemblies decreases with continuous increase of CTAB concentration, the CD signals of GNRs decrease obviously because of the reduction of hot spots from coupling of the GNRs. Nevertheless, such a rich plasmonic CD response in GNR assemblies is very surprising and unexpected, pushing us to explore the intrinsic relation between the chiroptical properties and the assembly mode that is ignored by other spectral analysis.

The question that we should first answer is whether the conformation modulated plasmonic response of the GNR assemblies is a universal phenomenon. Thus, both building blocks (CYS and GNR) are intentionally changed. When D-CYS is used to assemble GNRs with the aspect ratio of ∼2.2, the same conformation transition mediated by CTAB concentration is found, and the plasmonic CD response of the D-CYS assembled GNRs exhibits the mirror symmetry with that of the L-CYS assembled GNRs (Figure S3). In addition, under the control of surfactant concentration, the identical transition of the assembly modes is achieved with GNRs having larger aspect ratios of ∼2.9 and ∼3.4 (Figures S4−S9). When the aspect ratio of GNRs increases, the bisignated CD bands show gradual bathochromic shift, due to the red shift of the LSPR absorption (Figure 3a,b). Meanwhile, the plasmonic CD intensity of both EE and SS

dx.doi.org/10.1021/ja506790w | J. Am. Chem. Soc. 2014, 136, 16104−16107

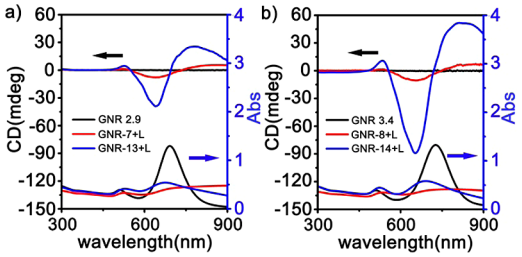

Figure 3. Comparison of optical properties of EE and SS assembled GNRs with aspect ratio of (a) ~2.9 and (b) ~3.4. The numbers in the labels represent the aspect ratio, for instance, "GNR 2.9" stands for GNRs with aspect ratio of ~2.9.

assembled GNRs is improved, partly resulting from the significant enhancement of the electromagnetic field around the GNRs of larger aspect ratios.[16] Two important conclusions can be further drawn by the quantitative comparison: (1) For GNRs of a certain aspect ratio, the *g* factor ratio of the SS vs EE assemblies (defined as the enhancement factor) is almost the same for the TSPR (Table S2) and LSPR bands (Table 1), highlighting that the conformation modulated CD response is general and applicable for both plasmon modes in GNRs. (2) As the aspect ratio of GNRs increases, the CD enhancement of the SS assemblies is much more evident (Tables 1 and S2), suggesting that the enhancement effect of the SS assembly against the EE assembly becomes larger with the increase of the aspect ratio.

The next question is the origin of the conformation modulated CD response of GNR assemblies. The first possibility is the formation of spatial chirality by the SS oriented GNR pairs, because spontaneous twisting of one nanorod against the other might break the centrosymmetric nature of the parallel assemblies.[11c,17] However, this hypothesis is excluded by a couple of experimental evidences. Representative 3D cryo-TEM images of SS GNR assemblies show that no fixed dihedral angles form between the adjacent SS GNR pairs (Figure S10). Moreover, when both achiral 3-mercaptopropionic acid and racemic DL-CYS molecules are used to assemble GNRs, neither the EE nor the SS assembly of GNRs shows the detectable CD response (Figure S11). The other possibility is that the plasmonic CD amplification is caused by the stronger hot spots in the gap of the SS GNRs. It is well-known that the physical mechanism of surface-enhanced Raman spectroscopy (SERS) comes from amplification of electromagnetic field at the plasmonic hot spots of noble metal NPs.[18] So the SERS spectra of both SS and EE assemblies are recorded to compare the electromagnetic effect in the assemblies, and the intensity of C−S stretching vibration of L-CYS molecules is chosen as a standard (Figure S12). It is clear that the SERS intensity of both EE assemblies and SS assemblies increases with the aspect ratio of GNRs, which is caused by the stronger electromagnetic field of GNRs with larger aspect ratio. Interestingly, on the contrary to the conformation modulated plasmonic CD response, the SERS intensity of EE GNR assemblies is even larger than that of SS GNR configuration (Table S3). This is mainly caused by the larger local field enhancement as well as more adsorbed CYS molecules in the EE assemblies (Table S1).[6c,19] The SERS measurement discloses that in addition to the electromagnetic field, there must exist an unexplored and major factor contributing to the distinct plasmonic CD signals for GNRs assembled in different modes.

Since the plasmonic CD signal is highly conformation-dependent, geometrical parameters related to the different assembly modes are destined to be the breakthrough point (Scheme 1). Discrete dipole approximation method is used to

Scheme 1. Diagram of the GNRs Assembled in Different Geometries, Showing the Important Parameters in the Theoretical Simulation[a]

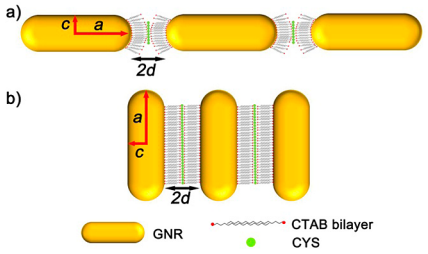

[a] *a* is the half length of GNRs, *c* is the half diameter of GNRs, and *d* is the half distance between the surfaces of the adjacent GNRs.

calculate the plasmonic CD signal for both the SS and EE assembled GNRs and to explain the conformation modulated CD response. In our system, we consider the basic unit of the GNR assemblies as the complex incorporating the dipole of CYS and the dipole at the center of GNR for either LSPR or TSPR. The dominant contribution of CD comes from the CYS-induced plasmonic CD of GNR. The CD signal of GNR is given by the difference of optical absorption (Q_{GNR}) between left/right circularly polarized field, that is, $CD_{GNR} = Q^{L}_{GNR} - Q^{R}_{GNR}$, where

$$Q^{L/R}_{GNR} \propto \int dV(\vec{E}_0 + \vec{E}^{L/R}_D)^* \cdot (\vec{E}_0 + \vec{E}^{L/R}_D) \quad (1)$$

$$\vec{E}^{L/R}_D(\vec{r}, \vec{r}_D) = G(\vec{r}, \vec{r}_D) p^{L/R}_D(\vec{r}_D) \quad (2)$$

In eq 2,

$$\vec{p}^{L/R}_D = \alpha^{L/R} \vec{E}_C n_{CYS} \quad (3)$$

where $\vec{E}_0$ is the incident field and $\vec{E}^{L/R}_D$ is the induced field due to CYS, $\vec{E}_0 + \vec{E}^{L/R}_D$ is the local field on GNR, $\vec{r}$ and $\vec{r}_D$ are the position coordinate for GNR and CYS, $\vec{p}^{L/R}_D$ is the dipole of CYS (at $\vec{r}_D$) for left/right circularly polarized field, where n_{CYS} is the number of CYS molecules in the gap (Table S1), $\vec{E}_C$ is the local field on CYS, and $\alpha^{L/R}$ refers to the polarizability for left/right circularly polarized field. Therefore, we obtain the following equations:

$$CD_{GNR} = A \cdot n_{CYS} \cdot \mathrm{Re}[\Delta\alpha \cdot \vec{E}^*_0 \cdot \vec{E}_C \cdot G(\vec{r}_0, \vec{r}_D)] \quad (4)$$

where $\Delta\alpha = \alpha^L - \alpha^R$, $G(\vec{r}_0, \vec{r}_D) \propto 1/|\vec{r}_0 - \vec{r}_D|^3$ ($\vec{r}_0$ is the center of GNR) in the dipole approximation, and A is a constant.

Crucially, considering the anisotropic dimension of GNR (Figure S13 and Table S4), the dipole−dipole distance (distance between CYS center and GNR center) is considerably different in the EE mode and SS mode (Scheme 1). Therefore, the anisotropic factor (AF_{SS} and AF_{EE}) of the SS and EE configuration is given by

$$AF_{SS} = \bar{A}/(c + d)^3, \quad AF_{EE} = \bar{A} \cdot q/(a + d)^3 \quad (5)$$

where $\bar{A} \propto A \cdot \Delta\alpha \cdot n_{CYS} \cdot E_C$, c and a are the half length of short and long axis, respectively, d is the half distance between the

dx.doi.org/10.1021/ja506790w | J. Am. Chem. Soc. 2014, 136, 16104−16107

surface of the adjacent GNRs, and q takes account of the multipole correction (since $a \gg d$), the n_{CYS}, and the gap field difference in the EE and SS configurations. Finally, using the consistent fitting parameter $\bar{A}$, one can theoretically calculate the enhancement factor of the SS configuration against the EE configuration at both LSPR and TSPR. For example, the enhancement factor at LSPR is 2.07, 3.90, and 5.65 for GNRs with aspect ratio of 2.2, 2.9, and 3.4, respectively (Part S3 in SI and Table 1).

Impressively, the theoretical results about the enhancement factors are in good agreement with the experimental observations (Tables 1 and S2), and important conclusions now can be clearly acquired. As shown in eq 5, the ratio, AF_{SS}/AF_{EE}, is inversely proportional to the cube of the dipole−dipole distance ratio ($AF_{SS}/AF_{EE} = R_{EE}^3/(q \cdot R_{SS}^3)$, $R_{SS} = c + d$ (or $R_{EE} = a + d$) is the dipole−dipole distance in SS (or EE) assembly, and q is a constant in calculation). Obviously, R_{SS} is smaller than R_{EE}, leading to the conformation modulated CD enhancement. With increase of the aspect ratio, AF_{SS}/AF_{EE} increases due to the decrease of c and simultaneous increase of a (Figure S13 and Table S4). It should be noted that seen from the SERS signal (Figure S12 and Table S3), the larger electromagnetic field effect is observed in the EE configuration than that in the SS configuration, which affects the CD signal in opposite way. Altogether, the plasmonic CD signal of GNR assembly is the superposition of the contribution from both the electromagnetic field effect at the "hot spots"and the geometry-dependent electromagnetic interaction. The dominant role of the conformation modulated electromagnetic interaction leads to larger CD signal of the SS assembled GNRs than that of the EE assembled GNRs, which is further amplified with increase of the aspect ratio of GNRs.

In conclusion, conformation-dependent plasmonic CD enhancement in the nanoassemblies is explored in this work, and such plasmonic CD enhancement could be further amplified through altering the aspect ratio of the building blocks. It is worth mentioning that the found plasmonic CD enhancement phenomena cannot be explained by the existent mechanism that is valid in many usual experiments. Detailed experimental and theoretical results disclose that the conformation-dependent dipole−dipole distance in the anisotropic assembly units is the crucial factor to generate the distinct plasmonic CD signals, which is not well recognized in the previous studies on CD enhancement. Our work lays the foundation to achieve tunable and intense plasmonic CD responses via construction of the nanoassemblies with varying shaped building blocks, which will have many potential applications in plasmonic devices and chiral sensing.

■ ASSOCIATED CONTENT

Supporting Information

Experimental results, theoretical calculations, and additional figures. This material is available free of charge via the Internet at http://pubs.acs.org.

■ AUTHOR INFORMATION

Corresponding Authors

zytang@nanoctr.cn
zhang_wei@iapcm.ac.cn

Notes

The authors declare no competing financial interest.

■ ACKNOWLEDGMENTS

This work was supported by National Basic Research Program of China (2014CB931801, Z.Y.T.; 2011CB922204, W.Z.), NSFC for Distinguished Youth Scholars (21025310, Z.Y.T.), NSFC (21475029, Z.Y.T.; 11174042, 11374039, W.Z.).

■ REFERENCES

(1) (a) Berova, N. N., Nakanishi, K., Woody, R. W. *Circular Dichroism: Principles and Applications*, 2nd ed.: Wiley-VCH: New York, 2000. (b) Fasman, G. D. *Circular Dichroism and the Conformational Analysis of Biomolecules*; Plenum: New York., 1996.

(2) (a) Ben-Moshe, A.; Maoz, B.; Govorov, A. O.; Markovich, G. *Chem. Soc. Rev.* **2013**, *42*, 7028. (b) Lieberman, I.; S, G.; Fried, T.; Kosower, E. M.; Markovich, G. *Angew. Chem., Int. Ed.* **2008**, *47*, 4855. (c) Wang, Y.; Xu, J.; Wang, Y. W.; Chen, H. Y. *Chem. Soc. Rev.* **2013**, *42*, 2930.

(3) (a) Govorov, A. O. *J. Phys. Chem. C* **2011**, *115*, 7914. (b) Govorov, A. O.; Fan, Z. Y.; Hernandez, P.; Slocik, J. M.; Naik, R. R. *Nano Lett.* **2010**, *10*, 1374.

(4) (a) Querejeta-Fernández, A.; Chauve, G.; Methot, M.; Bouchard, J.; Kumacheva, E. *J. Am. Chem. Soc.* **2014**, *136*, 4788. (b) George, J.; Thomas, K. G. *J. Am. Chem. Soc.* **2010**, *132*, 2502. (c) Alivisatos, A. P.; Mastroianni, A. J.; Claridge, S. A. *J. Am. Chem. Soc.* **2009**, *131*, 8455.

(5) (a) Guerrero-Martínez, A.; Auguié, B.; Alonso-Gómez, J. L.; Džolić, Z.; Gómez-Graña, S.; Žinić, M.; Cid, M. M.; Liz-Marzán, L. M. *Angew. Chem., Int. Ed.* **2011**, *50*, 5499. (b) Kuzyk, A.; Schreiber, R.; Fan, Z. Y.; Pardatscher, G.; Roller, E. M.; Hogele, A.; Simmel, F. C.; Govorov, A. O.; Liedl, T. *Nature* **2012**, *483*, 311.

(6) (a) Gubler, U.; Bosshard, C. *Nat. Mater.* **2002**, *1*, 209. (b) Pendry, J. B. *Science* **2004**, *306*, 1353. (b) Peng, S.; McMahon, J. M.; Schatz, G. C.; Gray, S. K.; Sun, Y. G. *Proc. Natl. Acad. Sci. U.S.A.* **2010**, *107*, 14530. (c) Lee, A.; Andrade, G. F. S.; Ahmed, A.; Souza, M. L.; Coombs, N.; Tumarkin, E.; Liu, K.; Gordon, R.; Brolo, A. G.; Kumacheva, E. *J. Am. Chem. Soc.* **2011**, *133*, 7563.

(7) (a) Zhu, Y. Y.; Xu, L. G.; Ma, W.; Xu, Z.; Kuang, H.; Wang, L. B.; Xu, C. L. *Chem. Commun.* **2012**, *48*, 11889. (b) Henzie, J.; Andrews, S. C.; Ling, X. Y.; Li, Z. Y.; Yang, P. D. *Proc. Natl. Acad. Sci. U.S.A.* **2013**, *110*, 6640.

(8) Shukla, N.; Bartel, M. A.; Gellman, A. J. *J. Am. Chem. Soc.* **2010**, *132*, 8575.

(9) (a) Huang, P.; Lin, J.; Li, W.; Rong, P.; Wang, Z.; Wang, S.; Wang, X.; Sun, X.; Aronova, M.; Niu, G.; Leapman, R. D.; Nie, Z. H.; Chen, X. Y. *Angew. Chem., Int. Ed.* **2013**, *52*, 13958. (b) Song, J. B.; Zhou, J. J.; Duan, H. W. *J. Am. Chem. Soc.* **2012**, *134*, 13458.

(10) Auguié, B.; Alonso-Gómez, J. L.; Guerrero-Martínez, A.; Liz-Marzán, L. M. *J. Phys. Chem. Lett.* **2011**, *2*, 846.

(11) (a) Zhu, Z. N.; Liu, W. J.; Li, Z. T.; Han, B.; Zhou, Y. L.; Gao, Y.; Tang, Z. Y. *ACS Nano* **2012**, *6*, 2326. (b) Li, Z. T.; Zhu, Z. N.; Liu, W. J.; Zhou, Y. L.; Han, B.; Gao, Y.; Tang, Z. Y. *J. Am. Chem. Soc.* **2012**, *134*, 3322. (c) Zhu, Z. N.; Guo, J.; Liu, W. J.; Li, Z. T.; Han, B.; Zhang, W.; Tang, Z. Y. *Angew. Chem., Int. Ed.* **2013**, *52*, 13571.

(12) Sreeprasad, T. S.; Pradeep, T. *Langmuir* **2011**, *27*, 3381.

(13) Jain, P. K.; Eustis, S.; El-Sayed, M. A. *J. Phys. Chem. B* **2006**, *110*, 18243.

(14) Xiang, Y. U.; Wu, X. C.; Liu, D. F.; Li, Z. Y.; Chu, W. G.; Feng, L. L.; Zhang, K.; Zhou, W. Y.; Xie, S. S. *Langmuir* **2008**, *24*, 3465.

(15) Funston, A. M.; Novo, C.; Davis, T. J.; Mulvaney, P. *Nano Lett.* **2009**, *9*, 1651.

(16) (a) Jain, P. K.; Hooshmand, N.; El-Sayed, M. A. *J. Phys. Chem. Lett.* **2011**, *2*, 374. (b) Zuloaga, J.; Prodan, E.; Nordlander, P. *ACS Nano* **2010**, *4*, 5269.

(17) Ma, W.; Kuang, H.; Xu, L.; Ding, L.; Xu, C.; Wang, L.; Kotov, N. A. *Nat. Commun.* **2013**, *4*, 2689.

(18) (a) Moskovits, M. *Rev. Mod. Phys.* **1985**, *57*, 783. (b) Kneipp, K.; Kneipp, H.; Itzkan, I.; Dasari, R. R.; Feld, M. S. *Chem. Rev.* **1999**, *99*, 2957.

(19) Lee, A.; Ahmed, A.; dos Santos, D. P.; Coombs, N.; Park, J.; Gordon, R.; Brolo, A. G.; Kumacheva, E. *J. Phys. Chem. C* **2012**, *116*, 5538.